Enhancing Solid-Liquid Interface Thermal Transport using Self-Assembled Monolayers

Zhiting Tian[1], Amy Marconnet[2], and Gang Chen[*]

[*] *Department of Mechanical Engineering*

Massachusetts Institute of Technology, Cambridge, MA 02139, USA

[1] *Department of Mechanical Engineering*

Virginia Tech, Blacksburg, VA 24061, USA

[2] *Department of Mechanical Engineering*

Purdue University, West Lafayette, IN 47907, USA

Abstract

The thermal conductance across solid-liquid interfaces is of interest for many applications. Using time-domain thermoreflectance (TDTR), we measure the thermal conductance across self-assembled monolayers (SAMs), grown on Au, to ethanol. We systematically study the effect of different functional groups and the alkane chain length on the thermal conductance. The results show that adding this extra molecular layer can enhance the thermal transport across the solid-liquid interface. While the enhancement is up to 5 times from hexanedithiol, the enhancement from hexanethiol, undecanethiol and hexadecanethiol is approximately a factor of 2.

[*] *Corresponding author. Electronic mail: gchen2@mit.edu*

Interfacial thermal conductance has been a subject of fundamental and practical interest for many years. Conventionally, extra molecular layers at an interface add to the total thermal resistance network and reduce the thermal conductance, especially for solid-solid interfaces[1]. Chemical functionalization, however, has significant influence on the interface thermal conductance across solid-solid interfaces due to enhanced interfacial bonding[2]. Recent studies have shown that covalent chemical bonding at solid-solid interfaces using self-assembled monolayers (SAMs) can improve the interfacial thermal conductance[3]. Compared to solid-solid interfaces, the thermal conductance across solid-liquid interfaces has received limited attention. Better understanding of solid-liquid interfacial transport is important for different applications such as cancer treatment based on thermal therapeutics and nanoparticles[4], solar thermal heating[5], and colloids and nanofluids[6]. Experiments on the thermal conductance of solid-liquid interfaces typically employ suspensions of metal nanorods in water or organic solvents[7]. Although planar solid-liquid interfaces modified with hydrophilic and hydrophobic SAMs have been experimentally studied[8,9], there have been no controlled studies of solid-liquid interfaces with and without SAMs and they varied the SAM type as well as the SAM end group. In this work, we systematically study the dependence of the thermal conductance on the functional end groups for the same class of SAM, as well as the dependence on chain length. We show that the addition of the extra SAM layer between the planar Au layer and ethanol enhances thermal transport. Specifically, increasing chain length does not adversely impact the interfacial thermal conductance, while different functional end groups enhance the thermal conductance to different degrees.

Alkanethiol and alkanedithiol SAMs are formed on an Au surface using a standard wet chemical preparation method[10]. Specifically, 100 nm thick Au coated glass slides (purchased from Phasis Sàrl) are immersed in a dilute (~2 mM) ethanolic solution of the thiols (purchased from Sigma-Aldrich) for 18-24 hours at room temperature. Excess thiol molecules not bonded to the Au surface are removed by cleaning with ethanol and a nitrogen gun. Molecular schematics of the four different SAMs grown for this study are shown in Fig. 1. All the SAMs have an alkyl chain ($-(CH_2)_n-$) as a molecular backbone, a head group containing a sulfur atom which strongly bonds to the Au surface, and a terminal end group. Hexanedithiol and hexanethiol have the same alkane chain length but different functional groups (thiol group $-CH_2SH$ vs methyl group $-CH_3$). In contrast, hexanethiol, undecanethiol and hexadecanethiol have the same end group ($-CH_3$) but different alkane chain lengths.

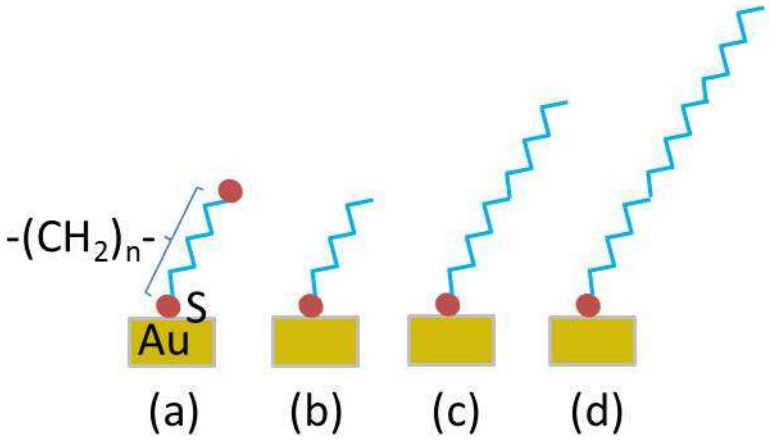

Fig. 1 Schematic of SAMs used in this study. (a) Hexenedithiol $SHCH_2(CH_2)_4CH_2SH$; (b) Hexanethiol $CH_3(CH_2)_4CH_2SH$; (c) Undecanethiol $CH_3(CH_2)_9CH_2SH$; and (d) Hexadecanethiol $CH_3(CH_2)_{14}CH_2SH$

For characterization of the thermal interface conductance between the Au surfaces and ethanol, the Au slides (with and without SAMs) are placed in contact with half of a demountable cuvette with a 1 mm thick channel, which is then filled with ethanol, as shown in Fig. 2. The Au film with a root mean square roughness of 0.8 nm, on which the SAMs are grown, serves as the transducer layer for optical time-domain thermoreflectance (TDTR) measurements of the interfacial thermal conductance. Details of the TDTR methodology can be found elsewhere [11,12]. In brief, a pulsed laser (~200 fs pulse-width, 80.7 MHz repetition rate) is used both as a heat source (pump beam) and thermal measurement tool (probe beam). The pump beam (400 nm wavelength), with a diameter of 60 μm, passes through the glass slide and is absorbed by the Au film. The variably time-delayed 12 μm diameter probe beam (800 nm wavelength), coaxial with the pump, measures the transient temperature relaxation following the pump pulse excitation by means of the change in reflectivity. The amplitude of the pump pulse train is modulated at 9 MHz to allow for lock-in detection of the thermoreflectance response. Although the estimated DC temperature rise is slightly above the ethanol boiling point, we did not observe bubble formation using a CCD camera either because the bubbles were too small or we had superheated ethanol. The pump power was limited to 30-35 mW to avoid observable bubble formation at the Au-ethanol interface while keeping the signal-to-noise ratio reasonably high. The sample properties, including the interface thermal conductance, impact the temperature decay curve and are extracted by fitting the data with a diffusive heat transfer model [11].

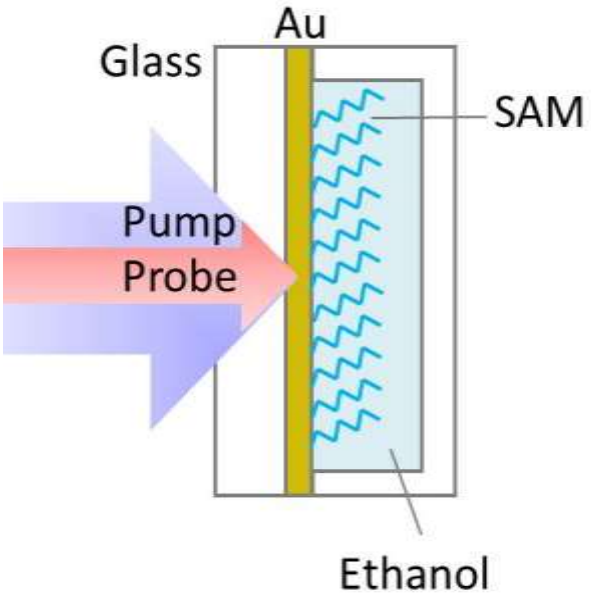

Fig. 2 Schematic of sample arrangement.

To measure the Au-ethanol interface thermal conductance (G), we first calibrate the thermal properties of the glass slide and ethanol using an as received Au-coated glass slide, which was cleaned and packaged in N_2 gas by the manufacturer. The thermal conductivity of the glass was determined by a standard TDTR measurement, where the pump and probe beams illuminate the Au side, and the thickness of the Au layer is treated as a known parameter, leaving the glass thermal conductivity and the Au-glass interface thermal conductance as the unknown parameters. The thermal conductivity of the ethanol was determined using TDTR, where the glass side is illuminated, and the unknown thermal parameters are the ethanol thermal conductivity and the Au-ethanol interface thermal conductance. The thermal conductivities of glass and ethanol are found to be k_{glass} = 1.25±0.02 W/mK and $k_{ethanol}$ = 0.17±0.01 W/mK, in good agreement with reference values [11,13], and the measured thermal conductance between glass and Au is $G_{Au\text{-}glass}$ = 51±2.6

MW/m^2K. These values are kept constant, and in all the subsequent data analysis, we only fit the interface thermal conductance between Au and ethanol for the samples with SAMs. All the difference in phase data between without SAM and with SAM is solely due to the existence of SAMs. The measured and fitted phase data are presented in Fig. 3 (a)-(d) for hexanedithiol, hexanethiol, undecanethiol and hexadecanethiol, respectively. The red dashed line denotes the thermal conductance value of the Au-ethanol interface without SAMs, $G_{Au\text{-}ethanol}$=17.7 ±3.7 MW/m^2K, which is comparable to that predicted by molecular dynamics simulations[14] of an Au-toluene interface ($G_{\text{Au-toluene}}$=13.8 MW/m^2K). For all samples with SAMs, the phase data clearly deviates from the red dashed line, illustrating an enhancement in thermal conductance of the Au-ethanol interface. Moreover, the phase data of hexanedithiol deviates more from the red dashed line than those of hexanethiol, undercanethiol and hexadecanethiol. The extent of enhancement, however, is challenging to quantify given that the measurement sensitivity decreases with increasing interfacial thermal conductance. Correspondingly, the fitted thermal conductance between Au and ethanol at room temperature are shown in Fig. 3(e). The error bars represent the propagation of uncertainties. The spot-to-spot variations are significantly less than the measurements uncertainty. The error bars represent the uncertainty in absolute magnitude of G, but we want to emphasize this experiment is truly a comparative measurement with and without the SAM layer. Once k_{glass}, $G_{Au\text{-}glass}$ and $k_{ethanol}$ are measured for a particular sample, the trend of enhanced thermal conductance by adding SAMs, and the hexanedithiol in particular yielding highest thermal conductance, holds even if these quantities are varied within the expected range.

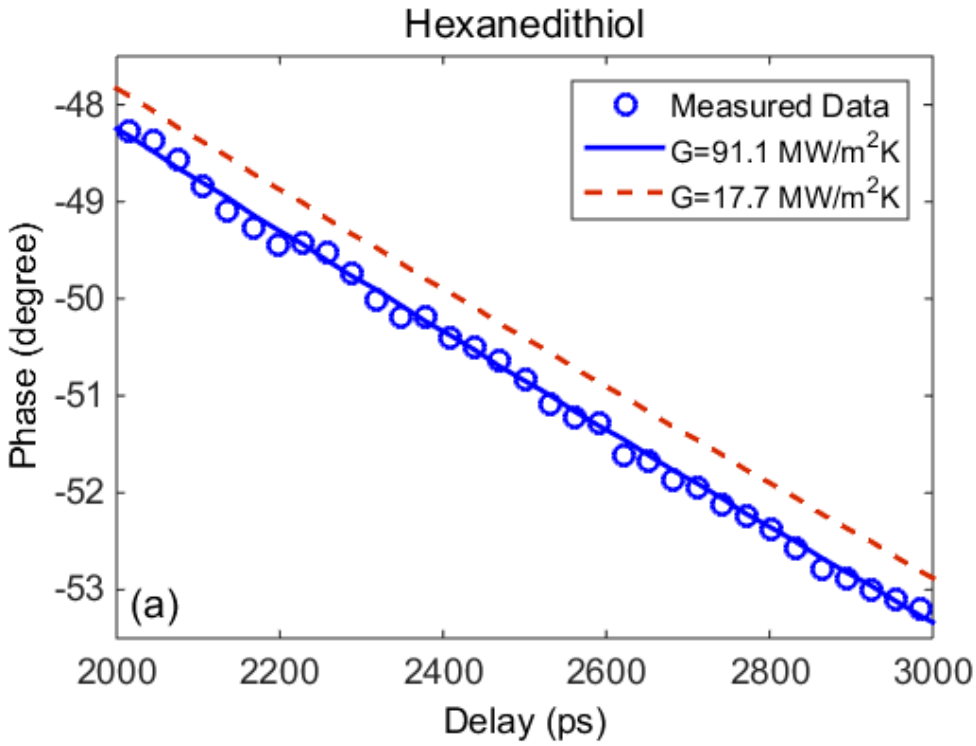

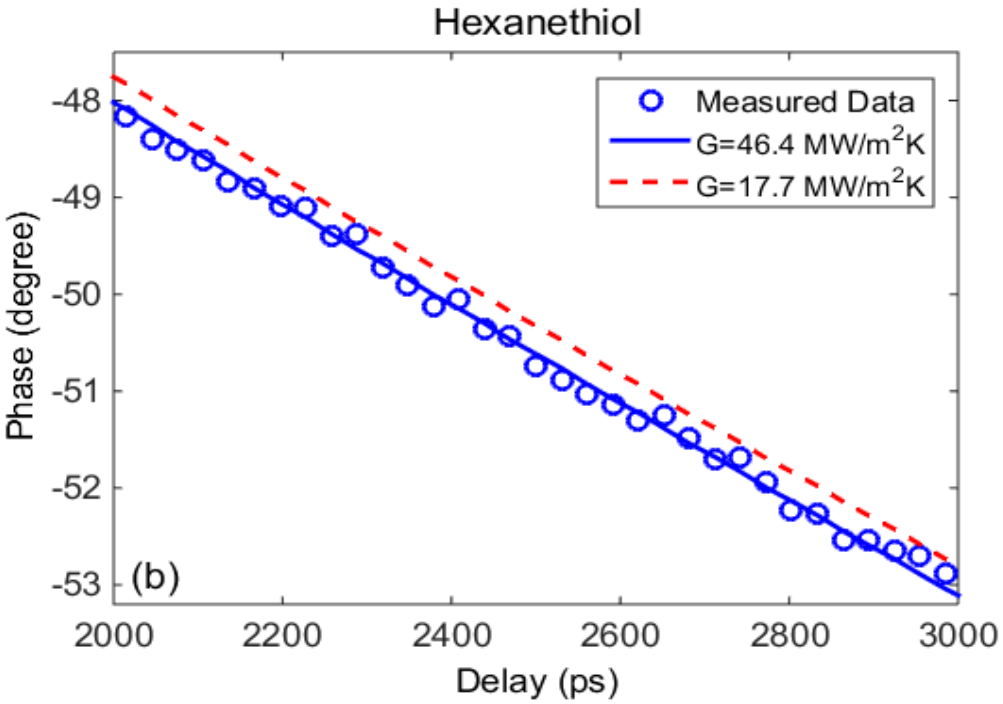

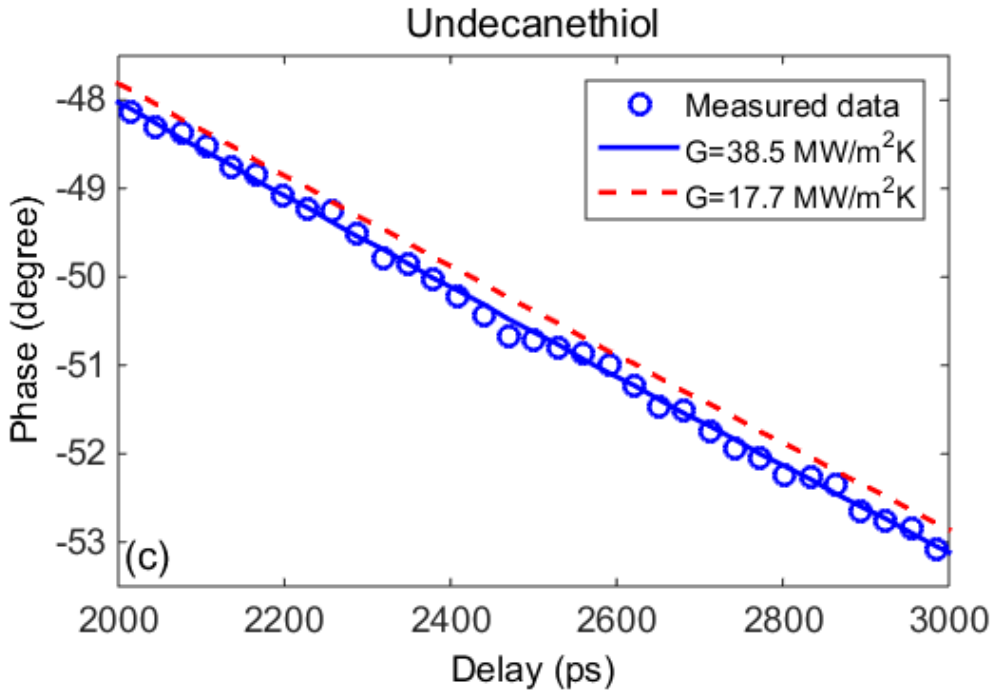

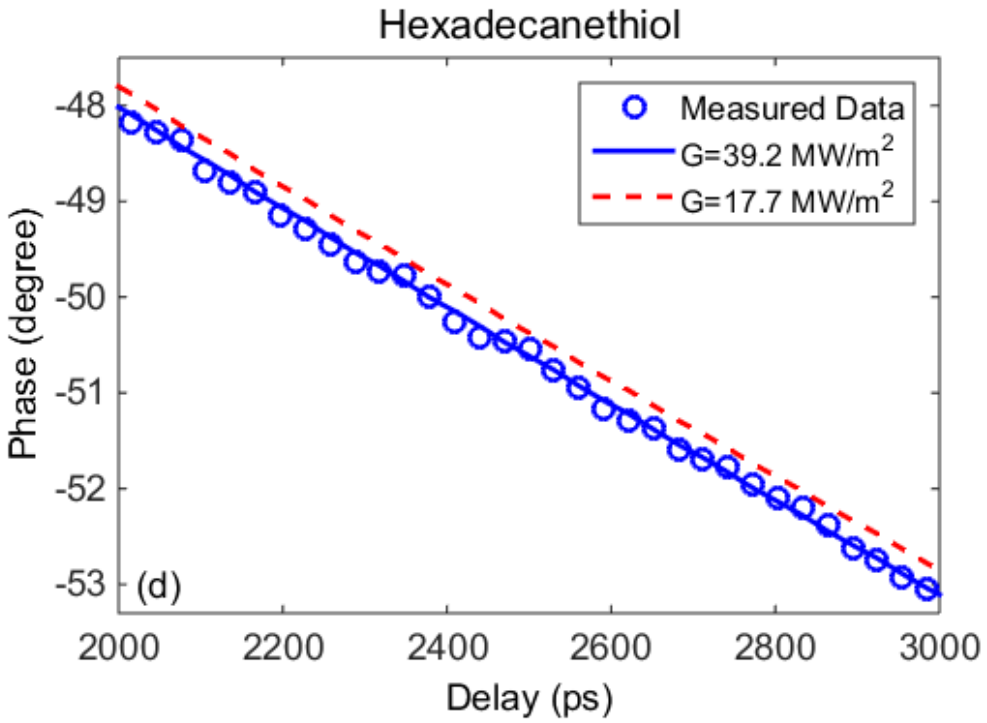

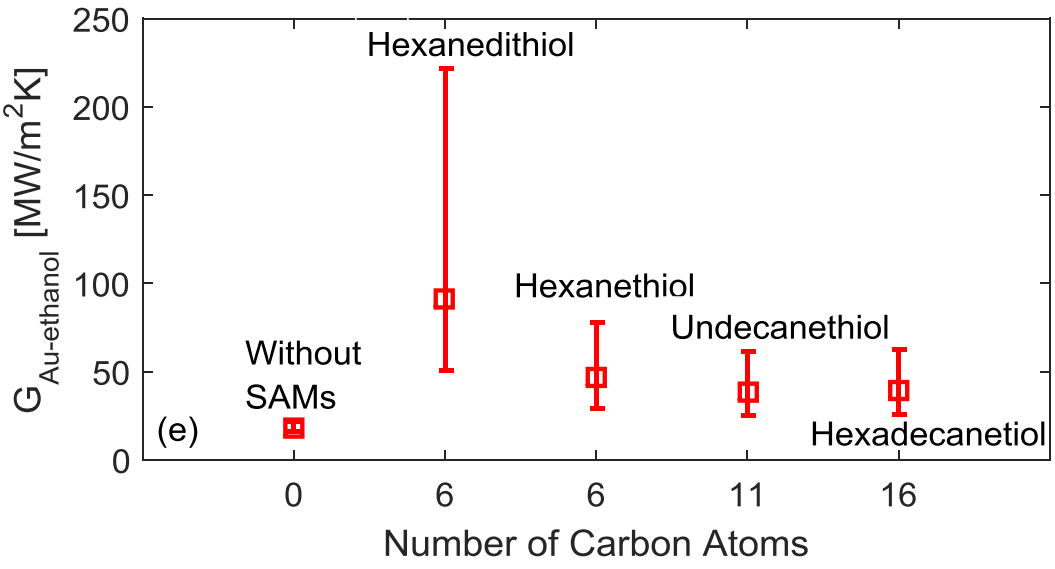

Fig, 3 The measured and fitted phase data for the Au-ethanol interface with (a) Hexanedithiol; (b) Hexanethiol; (c) Undecanethiol; and (d) Hexadecanethiol; The data are all fitted for the range of 500-3500 ps although only 2000-3000 ps portion is shown here to clearly demonstrate the difference. (e) Thermal conductance between Au and ethanol with and without SAMs from TDTR measurements at room temperature.

Counterintuitively, the interface conductance between Au and ethanol is improved by the existence of an extra molecular layer in all cases, as shown in Fig. 3 (e). While hexanedithiol improves the thermal conductance by a factor of ~5, hexanthiol, undecanethiol and hexadecanethiol all improve it by only a factor of ~2. Fundamentally, the thermal conductance at the interface depends on the transmission of vibrational modes (such as phonons) at the interface and a higher transmission leads to higher thermal conductance. Transmission depends on the stiffness of the springs on both sides of the interface as well as the springs connecting two sides of the interface. Therefore, both the spectra overlapping and stronger interfacial bonding are favorable to a higher thermal conductance. Compared with bare Au - ethanol interface, the improvement observed for all SAM-modified interfaces can be attributed to the stronger chemical bonds formed between Au and SAMs and between SAMs and ethanol, and the better matching of vibrational spectra. At one end of the molecular backbone, all the SAMs have a thiol group covalently bonded to the Au surface. At the other end, hexanedithiol has a thiol group exposed to the ethanol, while hexanethiol, undecanethiol and hexadecanethiol have a methyl functional group exposed to the ethanol. Since ethanol itself contains both a polar group (-OH) and a nonpolar methyl group, both the thiol end group and the methyl end group may form stronger chemical bonds with ethanol than the bare Au surface forms with the ethanol. Considering the vibrational spectra, previous simulation work [14,15] shows that the

vibrational spectra of alkanethiols are in between of the spectra of Au and organic solvent in the low frequency regime so the matching is better for SAM-modified interfaces. In other words, the SAMs serve as a bridge between Au and ethanol and facilitate thermal transport.

While the thermal conductance of the hexanedithiol SAM significantly exceeds the hexanethiol SAM, they differ only by the functional end group. The measured contact angles of ethanol on hexanethiol, undecanethiol and hexadecanethiol are 34º±4º, 35º±3º and 41º±2º respectively, while the contact angle on hexanedithiol is too small to be measured, as shown in Fig. 4. The contact angle can be related to the thermodynamic work of adhesion[9,16], the minimum work required to detach ethanol from the SAM. The smaller contact angle leads to the larger thermodynamics work of adhesion. In other words, the contact angle gives a measure of the bonding strength between the SAM and ethanol. Given that the vibrational spectra would not differ significantly among SAMs, the stronger bonding between hexanedithiol and ethanol than the other SAMs is expected to the dominant mechanism which leads to the higher thermal conductance. These results agree with earlier experiments, which showed that hydrophilic SAMs produced higher thermal conductance than hydrophobic SAMs for interfaces between water and metal [8,9].

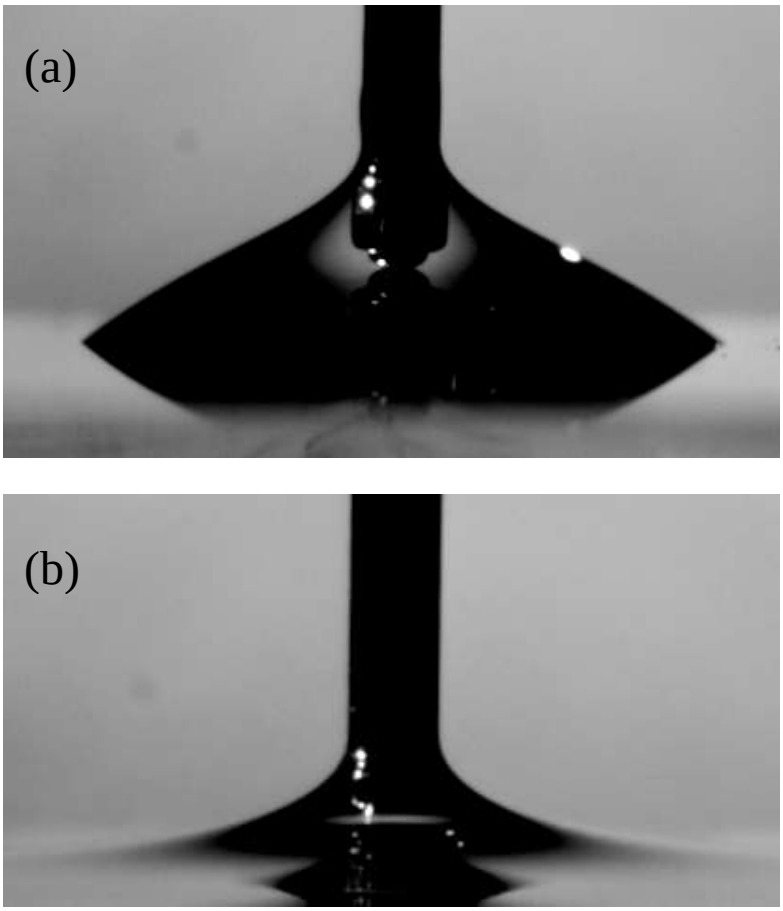

Fig. 4 Contact angles of ethanol on Au surface modified by (a) hexanethiol and (b) hexanedithiol SAMs.

We use optical spectroscopic ellipsometry to estimate the SAM thickness with a Cauchy model. The measured thicknesses for hexanethiol, undecanethiol and hexadecanethiol are 0.94±0.06 nm, 1.39±0.05 nm and 2.28±0.06 nm respectively, in good agreement with previous measurements on hexadecanethiol [17]. Despite the difference in chain length and film thickness, there is no observable difference in the thermal conductance for hexanethiol, undecanethiol and hexadecanethiol. This may indicate that phonon transport exhibits ballistic transport along the alkane chain, and that the phonon

vibrational spectra match regardless of the chain length investigated in this work. Ballistic transport is consistent with earlier experiments [1,9,18] and simulations [19] for solid-SAM-solid interfaces. Although one recent work[20] claimed length dependent thermal conductance over a wide range of molecular length ranging from n=2 to 18, the length dependence from n=6 to 16 at 300 K is rather weak.

In summary, we use TDTR measurements to investigate the thermal conductance between Au and ethanol with various interfacial SAMs. We show that the SAMs enhance the thermal transport from Au to ethanol. The interfacial thermal conductance is insensitive to the length of the alkane chain length, but strongly dependent on the functional group. Our results shed lights on strategies to further tune the interfacial conductance for practical applications.

The authors thank Kimberlee C. Collins and Maria Luckyanova for her help on the TDTR experiments, Emerald Ferreira-Yang for the SAM growth and Jun Xu for the ellipsometry measurements. This material is supported in part by Air Force Office of Scientific Research grant No. FA9550-11-1-0174 (for solid-liquid interface heat transfer) and by the "Solid State Solar-Thermal Energy Conversion Center (S3TEC)," an Energy Frontier Research Center funded by the U.S. Department of Energy, Office of Science, Office of Basic Energy Sciences under Award Number: DE-SC0001299/DE-FG02-09ER46577 (for the experimental system).

References

[1] R. Y. Wang, R. A. Segalman, and A. Majumdar, Applied Physics Letters **89** (17) (2006).

[2] P. E. Hopkins, M. Baraket, E. V. Barnat, T. E. Beechem, S. P. Kearney, J. C. Duda, J. T. Robinson, and S. G. Walton, Nano Letters **12** (2), 590 (2012); K. C. Collins, S. Chen, and G. Chen, Applied Physics Letters **97** (8) (2010).

[3] M. D. Losego, M. E. Grady, N. R. Sottos, D. G. Cahill, and P. V. Braun, Nature Materials **11** (6), 502 (2012).

[4] S. Lal, S. E. Clare, and N. J. Halas, Accounts of Chemical Research **41** (12), 1842 (2008).

[5] O. Neumann, A. S. Urban, J. Day, S. Lal, P. Nordlander, and N. J. Halas, Acs Nano **7** (1), 42 (2013).

[6] J. W. Gao, R. T. Zheng, H. Ohtani, D. S. Zhu, and G. Chen, Nano Letters **9** (12), 4128 (2009); R. T. Zheng, J. W. Gao, J. J. Wang, S. P. Feng, H. Ohtani, J. B. Wang, and G. Chen, Nano Letters **12** (1), 188 (2012); R. Prasher, P. E. Phelan, and P. Bhattacharya, Nano Letters **6** (7), 1529 (2006).

[7] J. Y. Huang, J. Park, W. Wang, C. J. Murphy, and D. G. Cahill, Acs Nano **7** (1), 589 (2013); J. Park, J. Y. Huang, W. Wang, C. J. Murphy, and D. G. Cahill, Journal of Physical Chemistry C **116** (50), 26335 (2012); A. J. Schmidt, J. D. Alper, M. Chiesa, G. Chen, S. K. Das, and K. Hamad-Schifferli, Journal of Physical Chemistry C **112** (35), 13320 (2008); O. M. Wilson, X. Y. Hu, D. G. Cahill, and P. V. Braun, Physical Review B **66** (22) (2002); Z. B. Ge, D. G. Cahill, and P. V. Braun, Journal of Physical Chemistry B **108** (49), 18870 (2004).

[8] Z. B. Ge, D. G. Cahill, and P. V. Braun, Physical Review Letters **96** (18) (2006).

[9] Hari Harikrishna, William A. Ducker, and Scott T. Huxtable, Applied Physics Letters **102** (25) (2013).

[10] J. C. Love, L. A. Estroff, J. K. Kriebel, R. G. Nuzzo, and G. M. Whitesides, Chemical Reviews **105** (4), 1103 (2005).

[11] A. Schmidt, M. Chiesa, X. Y. Chen, and G. Chen, Review of Scientific Instruments **79** (6) (2008).

[12] H. K. Lyeo and D. G. Cahill, Physical Review B **73** (14) (2006).

[13] N.B. Vargaftik, *Handbook of Physical Properties of Liquids and Gases: Pure Substances and Mixtures*. (Hemisphere Publishing Corporation, 1975).

[14] G. Kikugawa, T. Ohara, T. Kawaguchi, E. Torigoe, Y. Hagiwara, and Y. Matsumoto, Journal of Chemical Physics **130** (7) (2009).

[15] Gota Kikugawa, Taku Ohara, Tohru Kawaguchi, Ikuya Kinefuchi, and Yoichiro Matsumoto, Journal of Heat Transfer **136** (10), 102401 (2014).

[16] Natalia Shenogina, Rahul Godawat, Pawel Keblinski, and Shekhar Garde, Physical Review Letters **102** (15), 156101 (2009).

[17] F. Bordi, M. Prato, O. Cavalleri, C. Cametti, M. Canepa, and A. Gliozzi, Journal of Physical Chemistry B **108** (52), 20263 (2004).

[18] Z. H. Wang, J. A. Carter, A. Lagutchev, Y. K. Koh, N. H. Seong, D. G. Cahill, and D. D. Dlott, Science **317** (5839), 787 (2007).

[19] T. F. Luo and J. R. Lloyd, Journal of Heat Transfer-Transactions of the Asme **132** (3) (2010); J. C. Duda, C. B. Saltonstall, P. M. Norris, and P. E. Hopkins, Journal of Chemical Physics **134** (9) (2011).

[20] T. Meier, F. Menges, P. Nirmalraj, H. Hölscher, H. Riel, and B. Gotsmann, Physical Review Letters **113** (6), 060801 (2014).